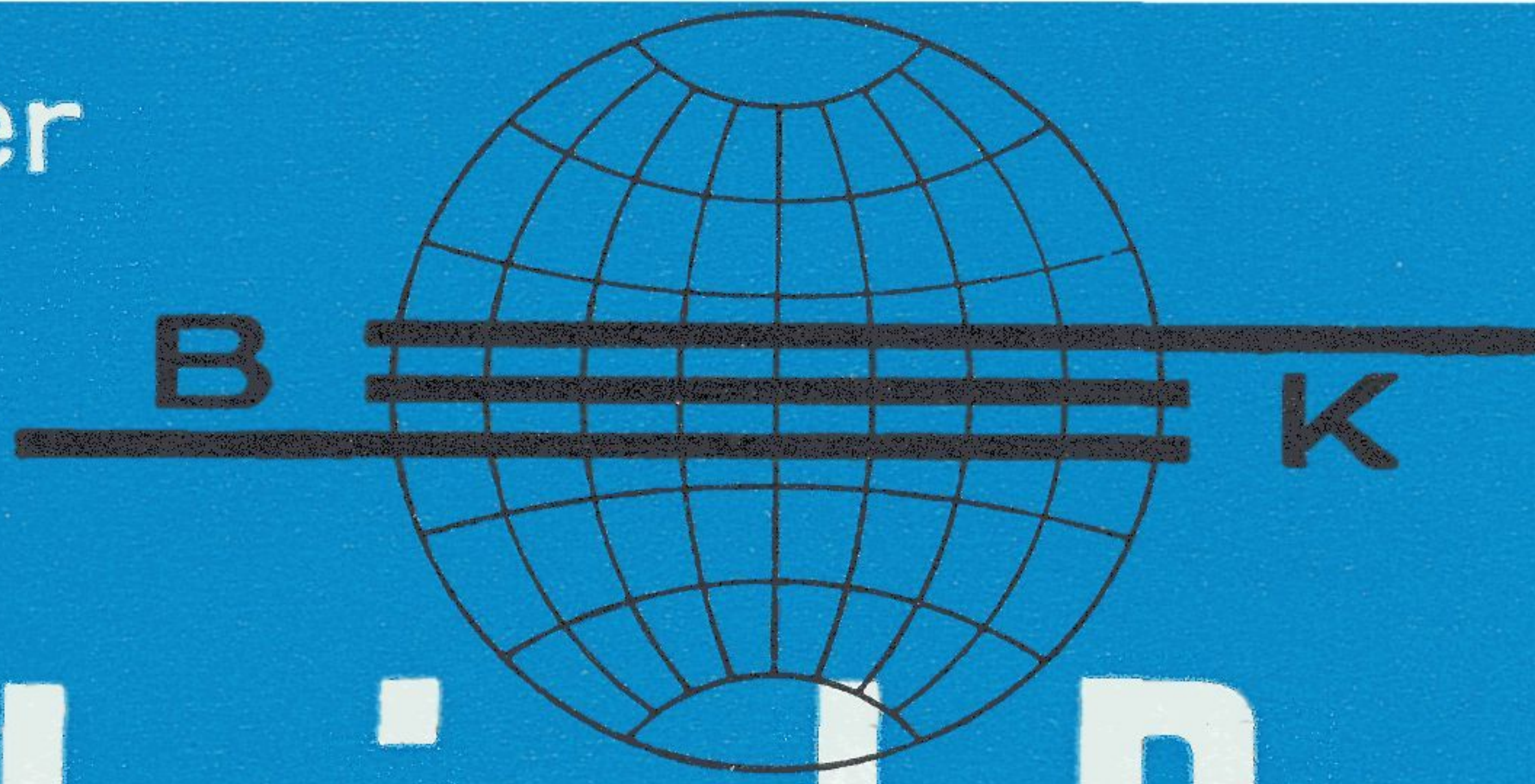


Brüel & Kjær



Technical Review

Teletechnical, Acoustical and Vibrational Research

A technical diagram showing a waveform on a grid. The waveform consists of four distinct pulses. A vertical double-headed arrow labeled 'a' indicates the peak-to-peak height of the pulses. A vertical double-headed arrow labeled 'b' indicates the height of the first pulse. A horizontal double-headed arrow labeled 'c' indicates the duration of one pulse. The diagram is set against a dark background with a light-colored grid.

MEASUREMENT

of the

COMPLEX

MODULUS OF ELASTICITY

**PREVIOUSLY ISSUED NUMBERS OF
BRÜEL & KJÆR TECHNICAL REVIEW:**

- 1-1954 Noise Measurements with the Audio Frequency Spectrometer Type 2109.
- 2-1954 The Automatic Analysis of Distortion in Sound Reproducing Equipment.
- 3-1954 Mobile Laboratories.
- 4-1954 Tube Measurements and Sound Insulation. Calibration of Probe-Tube Microphones.
- 1-1955 The Standing Wave Apparatus.
- 2-1955 Modern Accelerometers.
- 3-1955 Non Linearity of Condenser Microphones.
- 4-1955 A New Beat Frequency Oscillator Type 1014.
- 1-1956 Noise Measurements and Analyses.
- 2-1956 Use of Resistance Strain Gauges to determine Friction Coefficients.
- 3-1956 Determination of Acoustical quality of Rooms from Reverberation Curves.
- 4-1956 Electrical Measurements of Mechanical Vibrations.
- 1-1957 Strain Gauge Measurements.
- 2-1957 Sound Analysis in Industrial Processes and Production.
- 3-1957 Measurement on Tape Recorders.
- 4-1957 Measurements of Modules of Elasticity and Loss Factor for Solid Materials.
Surface Roughness Measurements.

COPIES AVAILABLE ON REQUEST

Measurements of the Dynamic Modulus of Elasticity and the Loss Factor for Solid Materials (Part II)

by A. SCHLÄGEL

SUMMARY

The practical application of the measuring methods dealt with in Technical Review No. 4-1957 is described and the measured result shown. A brief theoretical explanation of the methods is also given.

ZUSAMMENFASSUNG

Die praktische Anwendung der in Technical Review Nr. 4-1957 beschriebenen Messmethoden wird behandelt und einige Messresultate werden gegeben.

RESUME

L'application pratique des méthodes de mesure mentionnées dans le Technical Review no 4-1957 est décrite et quelques résultats de mesure sont montrés.

RESONANT METHODS

General.

A typical set-up for measuring the damping effect of coatings on metals is shown in fig. 14. The sample is suspended in two thin silk threads and is forced into vibrations by means of an electromagnet of the type used in ordinary telephone receivers. The electromagnet is fed from the Beat Frequency Oscillator Type 1014 and the vibrations are picked-up in the far end of the sample by another electromagnet similar to the one used for the excitation. The signal voltage from this "pick-up" is then fed to the Level Recorder Type 2304 via the Spectrometer Type 2109.

Because vibration damping coatings in the vast majority of cases are used on steel, it is natural to use a steel bar as sample. Steel is furthermore a very convenient material when working with magnetic forces. However, the use of electro-magnetic transducers do not set any limitation to the sorts of material which can be used as samples. In the case of non-magnetic materials small pieces of razor blades can be cemented onto the ends of the sample, without causing any effect on the measured results.

If the sample is suspended to vibrate with both ends free, it is very important that the supporting points are chosen exactly in the nodal points. If not, extra damping is introduced, and the results obtained are not correct.

Different methods can be used to determine the position of the nodal points of the vibrating sample. The best way is to cover the sample with a thin layer of moulding sand and turn the BFO to the n 'th allowed frequency of the bar. The nodal points are then the points where the sand remains. The n 'th

allowed frequency is to be considered as the frequency which makes the bar vibrate with $(n + 1)$ nodal points.

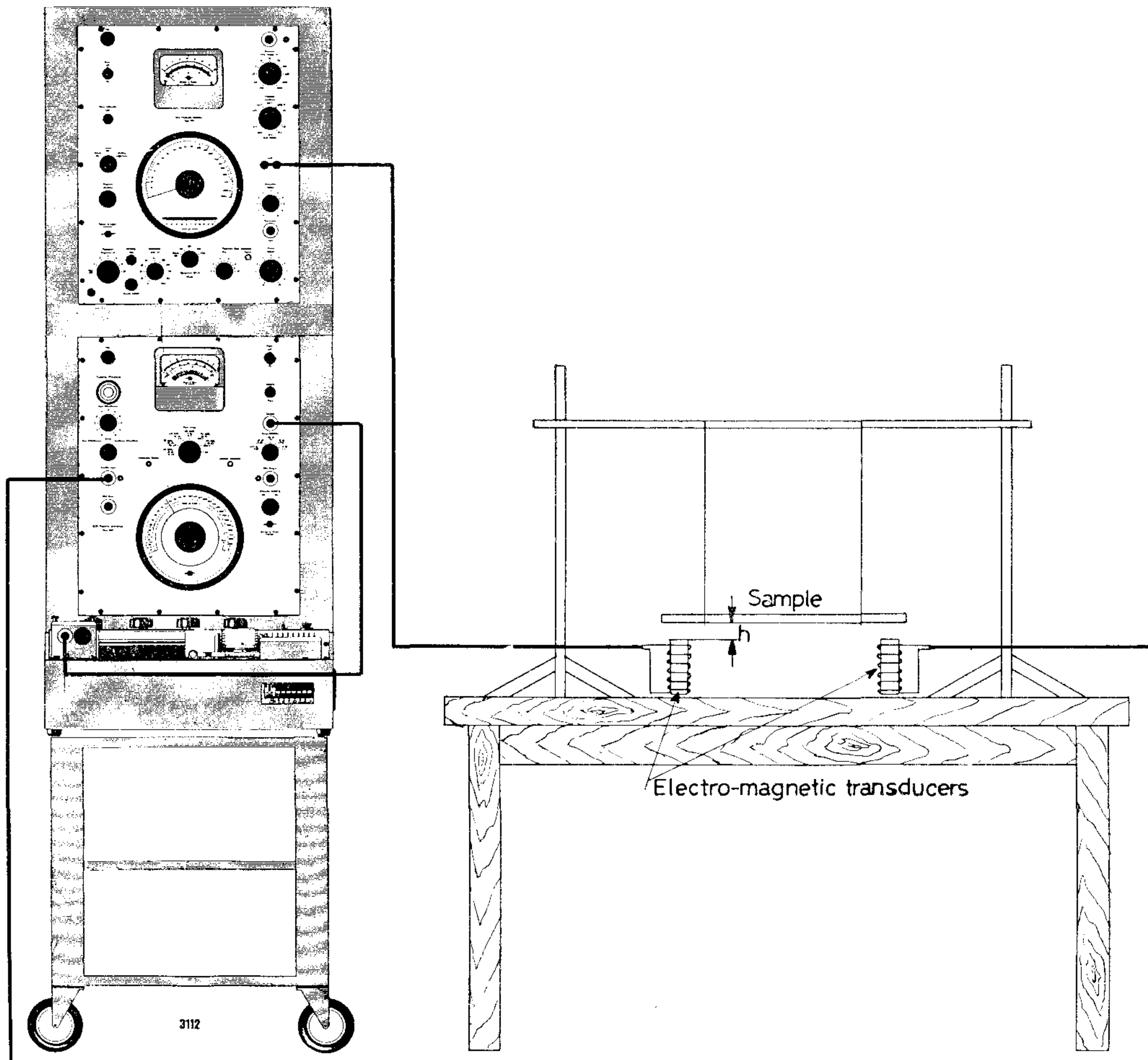


Fig. 14. Measuring set-up used for the resonant methods.

If the sample is homogeneous, the distance l_n from the end of the bar to the nearest nodal point may be calculated from the equation:

$$l_n = 0.66 \frac{l}{2n + 1}$$

where l is the length of the bar, and n is the order of the allowed frequency. Because this distance is a function of the allowed frequency, every resonance frequency requires its special suspension points to give correct measurements.

A. The Frequency Response Method.

In fig. 15 is shown a resonance-curve measured by means of the set-up described. The loss factor d is found from the formula:

$$d = \frac{\Delta f}{f} \quad (I)$$

To determine the influence on the loss factor of the distance h between the sample and the electromagnets a number of resonance-curves were recorded for different values of h . The results obtained are given in table I. It

Table I.

f_1 c/s	834	834	834	834	834	834
h mm	0.8	1.2	1.6	2.0	3.0	5.5
Δf c/s	0.25	0.24	0.25	0.17	0.17	0.17
$d \times 10^{-4}$	3.0	2.9	3.0	2.1	2.1	2.1

is seen that the distance should be at least 3 mm. Due to very low loss factors the bandwidths of the resonance peaks are small, causing a relatively big dispersion in the measured results. The method is therefore more convenient when measurements are carried out on materials with higher loss factors.

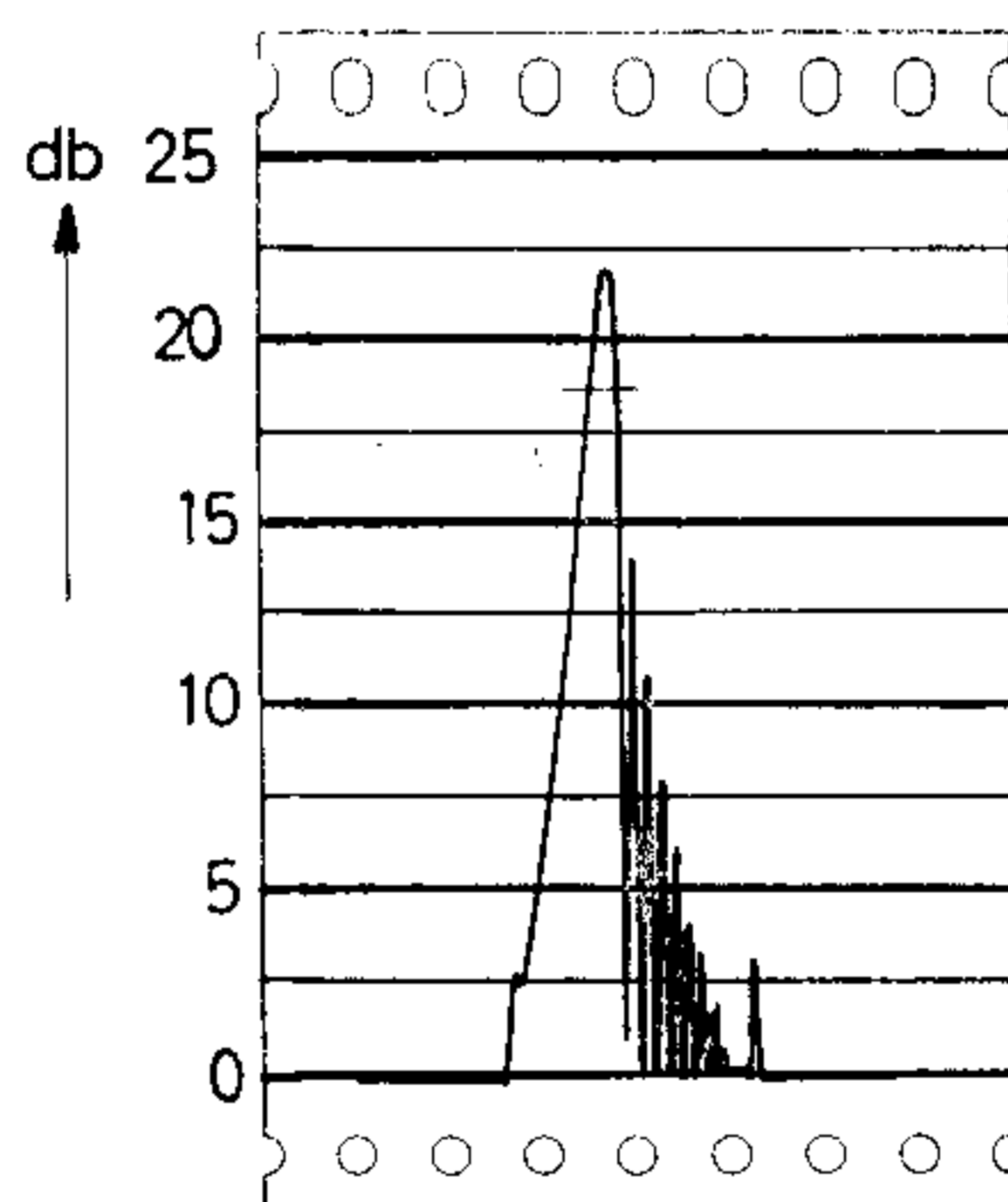


Fig. 15. Resonance-curve obtained by means of the set-up shown in fig. 14.

Fig. 16 shows the resonance curve (2) for such a material. It is furthermore shown that the measurement can be carried out selectively when the filter characteristic (1) of the employed filter is taken into consideration. From the figure is found $\Delta f = 38$ c/s and $f = 1,034$ c/s, and consequently

$$d = \frac{38}{1,034} = 33 \times 10^{-3}$$

B. The Reverberation Method.

An alternative to the frequency response method is the reverberation method. By pressing the "Oscillator Stop" switch on the BFO, using the same measur-

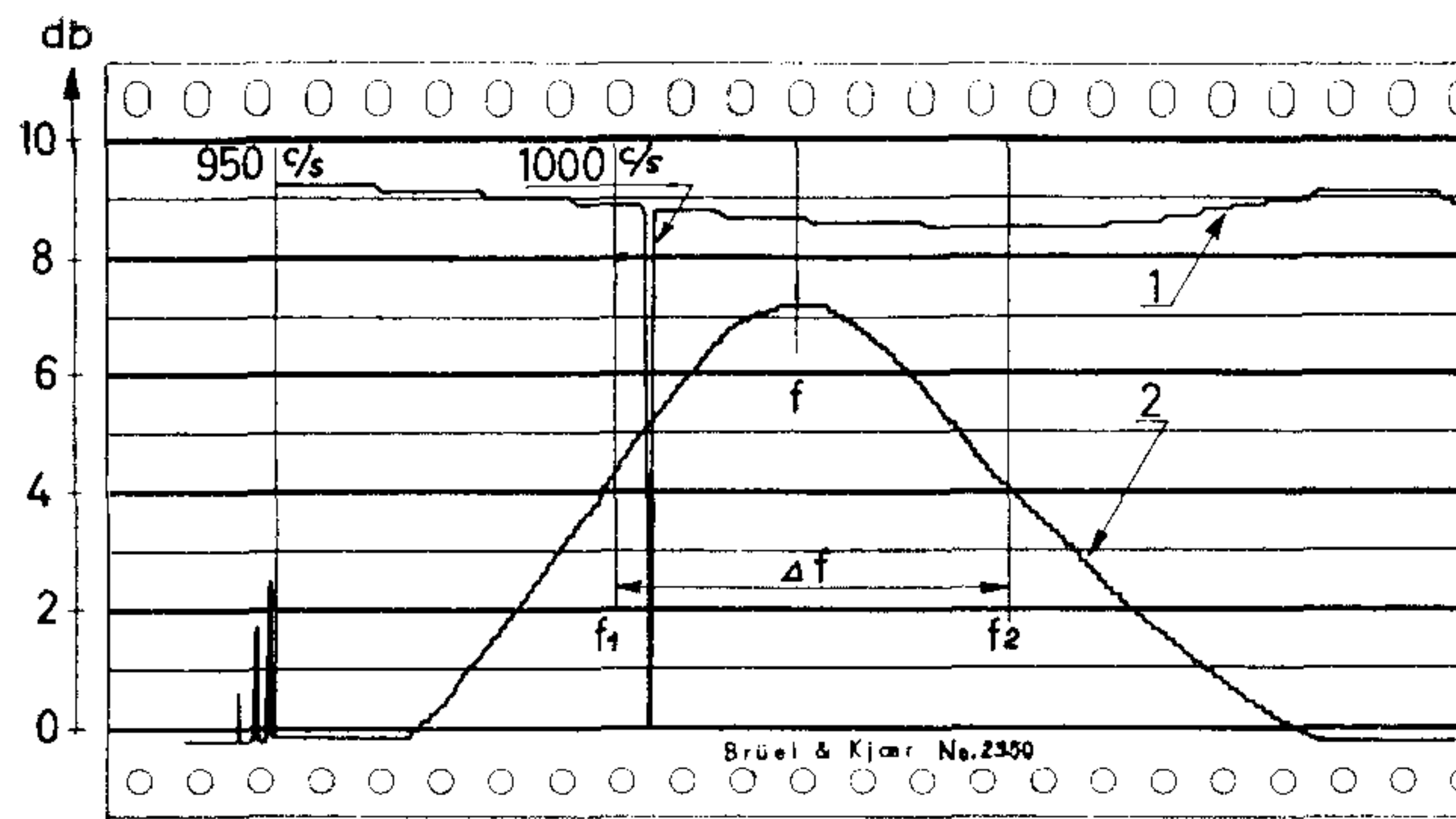


Fig. 16. Resonance-curve of a material with a high loss-factor.

ing set-up as for the frequency response method (fig. 14), the excitation of the sample is stopped and the decay of the vibration level recorded on the Level Recorder. To facilitate the calculation of the reverberation time from

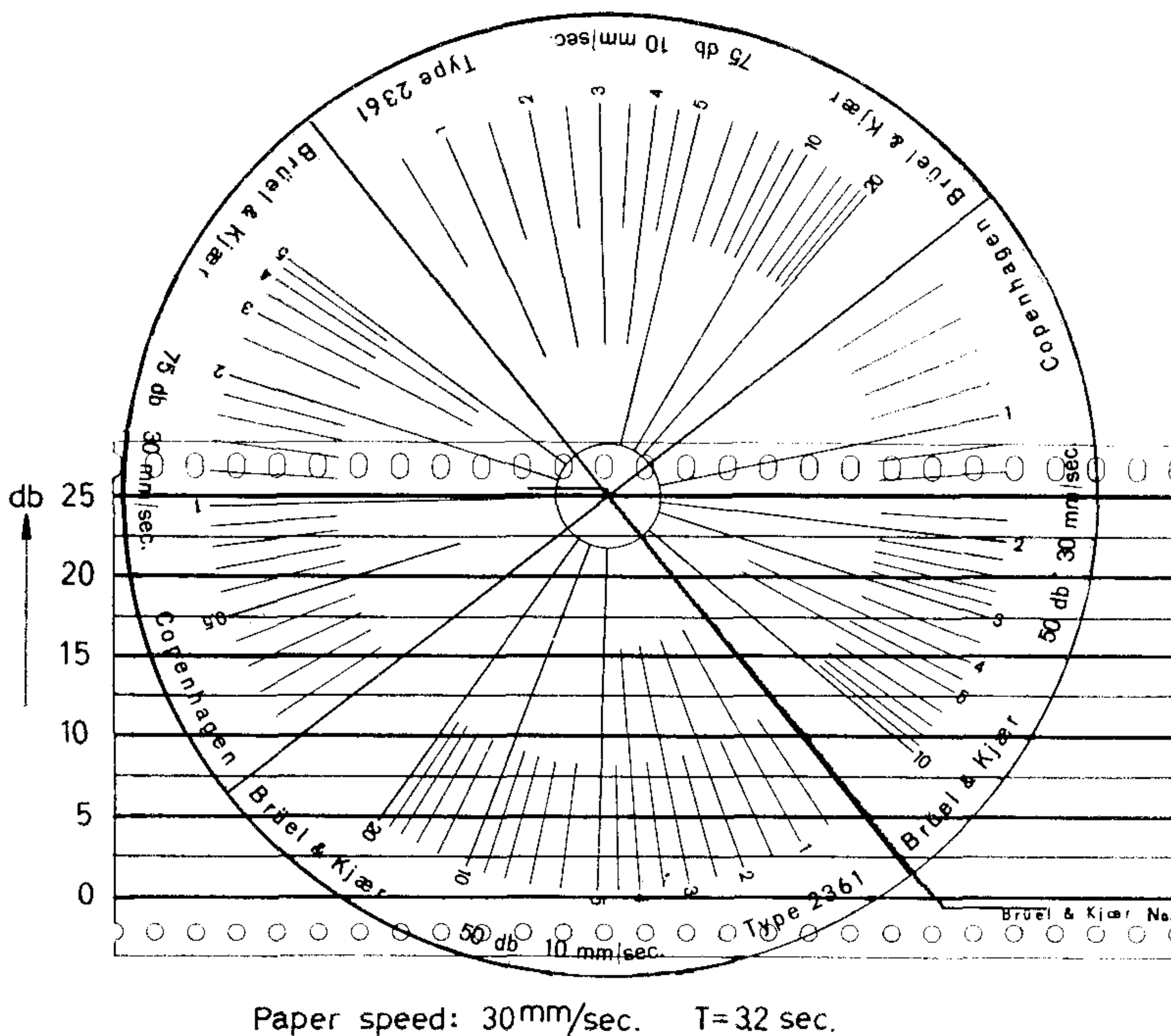


Fig. 17. The Protractor SC 2361 placed on a recording of a reverberation curve obtained by means of the set-up fig. 14.

the recording, the Reverberation Time Protractor SC 2361 can be used. The Protractor and a recording obtained with the set-up described is shown in fig. 17.

The Protractor itself is divided in 4 sections, marked 75 db 10 mm/sec., 75 db 30 mm/sec., 50 db 10 mm/sec., and 50 db 30 mm/sec., the letters referring to the actual potentiometer and paper speed to be used on the Level Recorder.

It is used by placing the thick line which indicates the *left* section line (the line closest to the B in Brüel & Kjær) over the recorded decay curve in such a way that one of the horizontal lines on the recording paper passes through the center of the Protractor, see also fig. 17. The reverberation time in seconds, based on a total decrease in level of 60 db, can then be read directly at the point where this horizontal line crosses the Protractor scale. From the recording it is seen that the reading is 1.6 sec. This value is only correct for a paper speed of 30 mm/sec. when used in connection with 50 db potentiometer. For the case in question a 25 db potentiometer was used, and the reading must consequently be multiplied by a factor 2. From the equation

$$d = \frac{2.2}{T \times f_n} \quad (\text{II})$$

the loss factor d is then found. T is the reverberation time in sec., and f_n the measuring frequency.

The measurement of the reverberation time can also be used to check the calculated value of the distance between the nodal points and the end of the sample. The longest reverberation time, i.e. the smallest loss, must be measured when the sample is suspended in its nodal points, and some reverberation curves have been recorded for different distances l_n . The dimensions of the sample used were:

Length: $l = 20$ cm, height: $q = 0.63$ cm, width: $b = 2.5$ cm

At the first allowed frequency ($n = 1$) the distance l_n is expected to be (see also the formula on p. 2).

$$l_n = \frac{0.66 \times 20}{2 + 1} = 4.4 \text{ cm}$$

The measured results shown in table II page 6 are in good accordance with the calculated value.

For both the frequency response method and the reverberation method, the real part of the dynamic modulus of elasticity is determined from

$$E' = \left(\frac{f_n}{\beta_n} \right)^2 \left(\frac{l^2}{q} \times 4 \pi \sqrt{3\rho} \right) \text{ dyne/cm}^2 \quad (\text{III})$$

If the values:

$n = 1$, $f_n = 834$ c/s, $\beta_n = 4.73$, $l = 20$ cm, $q = 0.63$ cm, and $\rho = 7.7$ g/cm³ are inserted, the modulus of elasticity is found to be

$$E' = 2.44 \times 10^{12} \text{ dyne/cm}^2$$

C. Method suitable for Small Test Objects.

The method to be described has been developed by Dr. G. W. Becker at Physikalisch Technisches Bundesanstalt, West Germany. The method is only suitable for measurements on small samples and requires therefore that the material of the test object has a high degree of homogeneity. Because this

Table II.

l_1 cm	4.1	4.2	4.3	4.4	4.5
T sec.	3.14	3.14	3.20	3.20	3.20

$$f_1 = 834 \text{ c/s}$$

method furthermore assumes that the sample is formed as a bar, it is especially useful for measurements carried out on high polymer materials. A sketch of the set-up employed for the measurements is shown in fig. 18. The bar-shaped sample is mounted vertically and is clamped in the upper end. It is forced into vibrations by means of an electromagnet placed at its free end, and the oscillations are picked up by another electromagnet placed between the free end and the clamping point. To keep the direct coupling

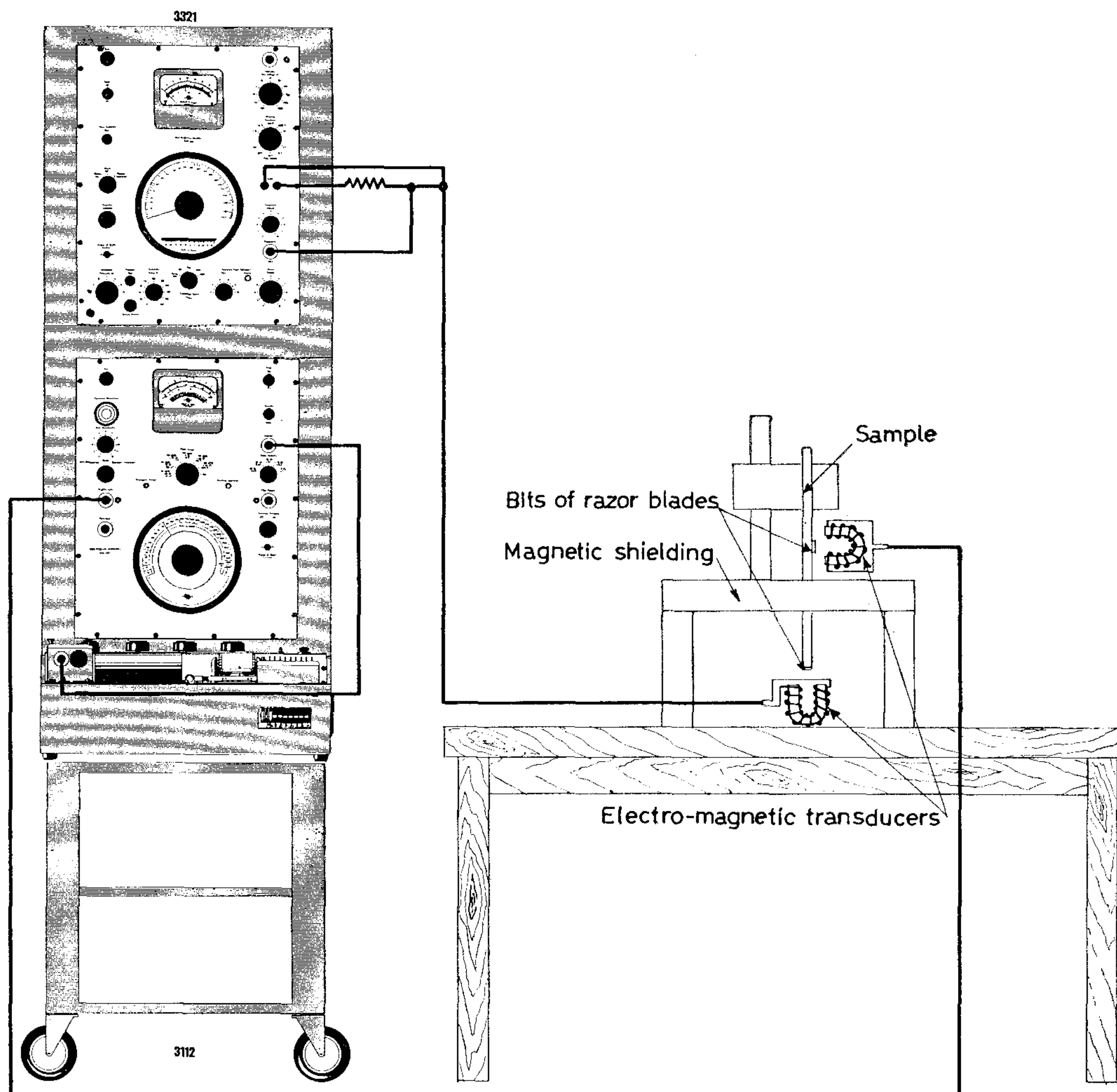


Fig. 18. Measuring arrangement used for testing small samples.

between the two electromagnets to a minimum a $\frac{1}{2}$ inches thick iron plate is mounted between them. When measurements are carried out on non-magnetic materials, small pieces of razor blades are cemented onto the sample, see fig. 18.

The exciting electromagnet is fed from the BFO. To keep a constant vibrating force independent of the frequency, the electromagnet is fed with constant current. This is obtained by keeping the voltage drop across a series-resistor constant by means of the compressor circuit of the BFO, see also fig. 18.

The signal from the electromagnet used as pick-up is fed to the Spectrometer and the Level Recorder.

Utilizing the possibility of synchronizing the BFO and the Level Recorder, an automatic recording can be made on pre-printed, frequency calibrated recording paper, covering the entire frequency range from 20 c/s to 20,000 c/s.

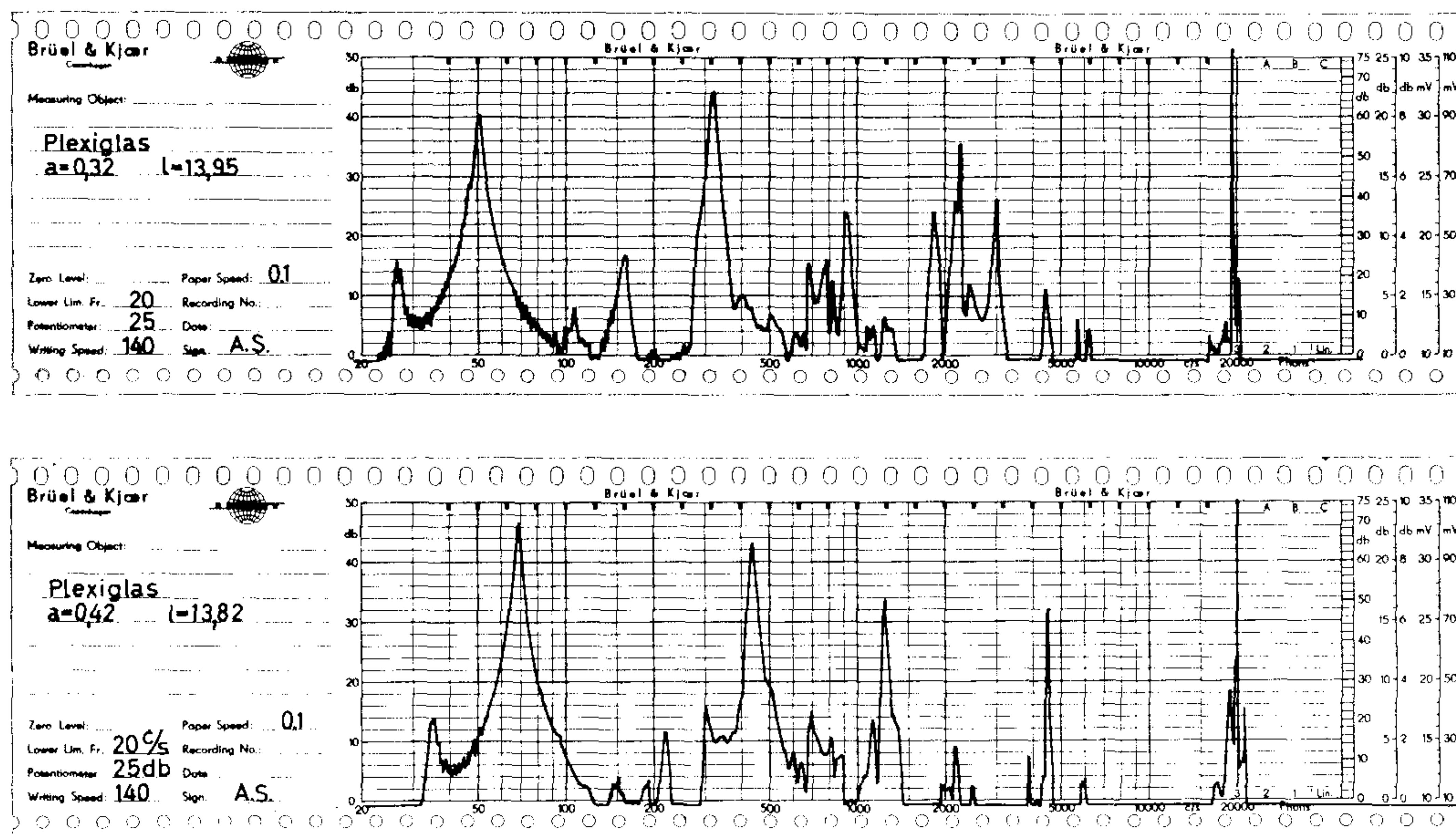


Fig. 19. Automatically recorded resonance curves of two plexiglas bars of different dimensions.

Measurements were then taken on two bar-shaped samples of plexiglas, an acrylic design. The dimensions of the bars from the clamping to the free end were:

1. $13.95 \times 0.32 \times 2.5$ (cm)
2. $13.82 \times 0.42 \times 2.5$ (cm)

and the recorded resonance-curves are shown in fig. 19.

The resonance curves may look a little confusing due to the many different peaks which are not all caused by "allowed" resonances of the sample. The following discussion will, however, make the recording easier to understand. Working with electro-magnetic transducers a certain amount of second harmonics is inevitable, therefore small peaks can be expected one octave below the allowed frequencies of the bar.

Further resonances due to the suspension system are also to be expected. They are readily found because they occur at the same frequencies independent of the length and thickness of the sample. In fig. 20 the two recordings from fig. 19 are shown, recorded on one piece of paper. By comparing the curves, the resonance frequencies of the suspension system are found as the peaks marked R.

Having eliminated the disturbant peaks only the ones marked 1, 2, 3, 4, 5, 6, and 7 remain. From these peaks the loss factor d and the real part of the modulus of elasticity E' is calculated by means of equation I and III respectively.

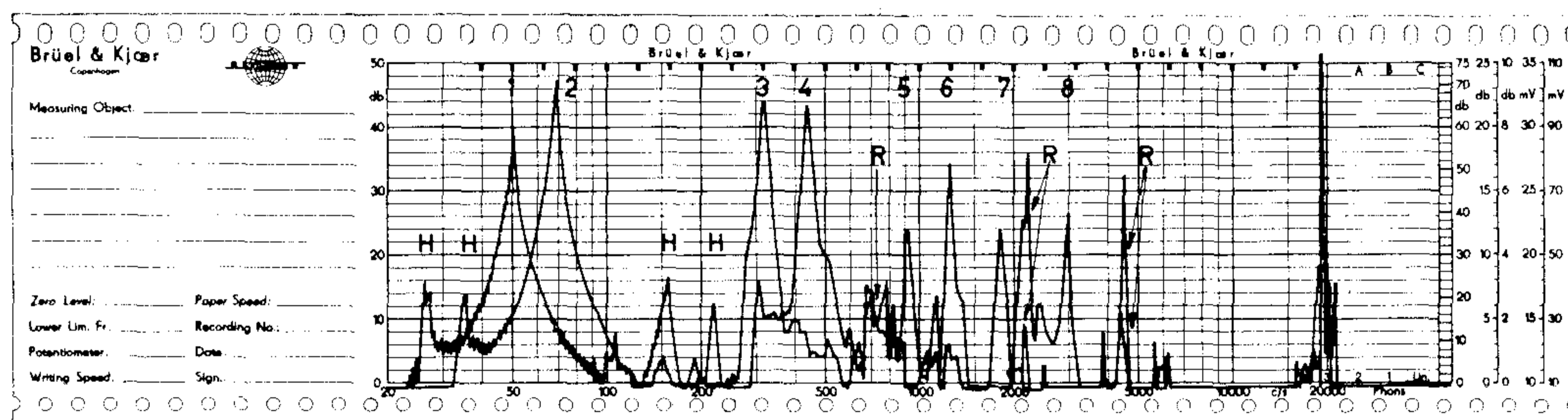


Fig. 20. The curves shown in fig. 19 recorded on one sheet of recording paper.

It is evident that a greater "peakwidth" would increase the accuracy of the loss factor calculation. To obtain this, the paper speed of the Level Recorder must be increased. This involves, however, that no recording paper with pre-printed frequency scale is available. It is thus necessary to mark certain frequencies as shown on the recordings fig. 21.

The value of the loss factor d and the real part E' of the dynamic modulus of elasticity calculated from the two curves are found in table III.

The expanded frequency scale technic can just as well be used over the entire frequency range of the Oscillator, a frequency mark at the start and one at the end of the curve being sufficient for a complete frequency calibration of the recording paper.

When measurements are taken on materials of this type a frequency scanning speed of 4 minutes per revolution of the Oscillator tuning capacitor is sufficiently slow. A check was made by lowering the scanning speed to 12 minutes per revolution. This caused no change in the height or width of the various resonance peaks.

It is also important to use correct writing speed on the Level Recorder. A speed of 140 mm/sec. was found to be convenient. A lower speed showed to have some, although very little, influence on the steepest peaks. A higher writing speed can be used, but the sensitivity of the set-up to irrelevant shocks, like banging doors etc., is then increased.

A 25 db potentiometer seems to be the one best suited for the dynamic range in question.

The features of the method described above, i.e. the relative uncritical suspension, the automatic frequency scanning, and the immediate recording, make it especially well suited for use in production control systems. Even unskilled personal will in a short time be able to quickly measure the response curve and calculate E' and d for a given sample.

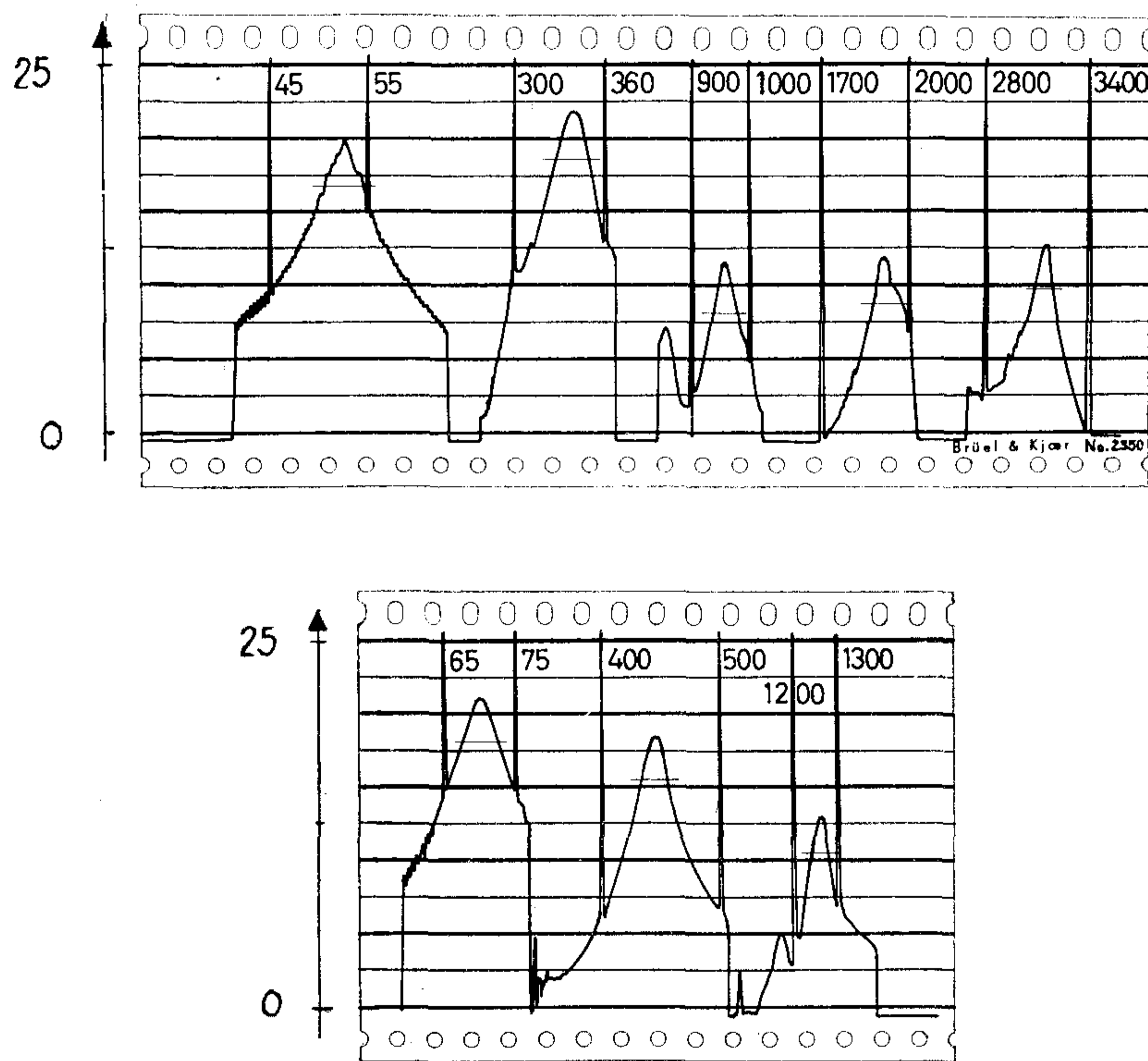


Fig. 21. The resonance-curves of two plexiglas bars recorded with extended frequency scale.

NON RESONANT METHODS

The measuring set-up used is shown in fig. 22. The sample, which must be a long, bar-shaped unit, is connected to the axis of a vibrating system as shown in the figure. Hanging vertically the lower end is stuck into a sand filled box. The vibrations are picked up by a displacement sensitive pick-up e.g. a pick-up of the same type as the one used in the Brüel & Kjær Roughness Meter Type 6100. This pick-up loads the sample with a static force of less than one gramme. A chain drive system which is driven from the motor in the Level Recorder enables the pick-up to be passed along the sample, see fig. 22.

The vibrations of the sample are controlled by the BFO, and the signal from the pick-up fed to the Spectrometer Type 2109 via the Preamplifier Type 1606. From the output bushing of the Spectrometer the signal is fed onto the Level Recorder. The Preamplifier features a very high input-impedance and is inserted to obtain a lower limiting frequency of the set-up

Table III.

n	β_n	f_n c/s	l cm	a cm	ρ g/cm ³	E' dyne/cm ²	Δf_n c/s	d
1	1.875	51	13.95	0.32	1.18	4.35×10^{10}	3.35	6.58×10^{-2}
2	4.694	334	13.95	0.32	1.18	4.64×10^{10}	20.7	6.19×10^{-2}
3	7.855	950	13.95	0.32	1.18	4.88×10^{10}	45.6	4.80×10^{-2}
4	10.99	1890	13.95	0.32	1.18	5.12×10^{10}	101.8	5.38×10^{-2}
5	14.13	3130	13.95	0.32	1.18	5.07×10^{10}	127.8	4.07×10^{-2}
1	1.875	69	13.82	0.42	1.18	4.43×10^{10}	5.10	7.38×10^{-2}
2	4.694	443	13.82	0.42	1.18	4.64×10^{10}	23.6	5.45×10^{-2}
3	7.855	1258	13.82	0.42	1.18	4.80×10^{10}	62.0	4.93×10^{-2}

of 20 c/s. If the Preamplifier is not used, i.e. the signal is fed directly to the Spectrometer, the lower limiting frequency will be approx. 100 c/s. The measurements were now carried out by exciting the system at an arbitrary, pre-chosen frequency and setting the filter switch of the Spectrometer to a filter, the passband of which contained this frequency. Using

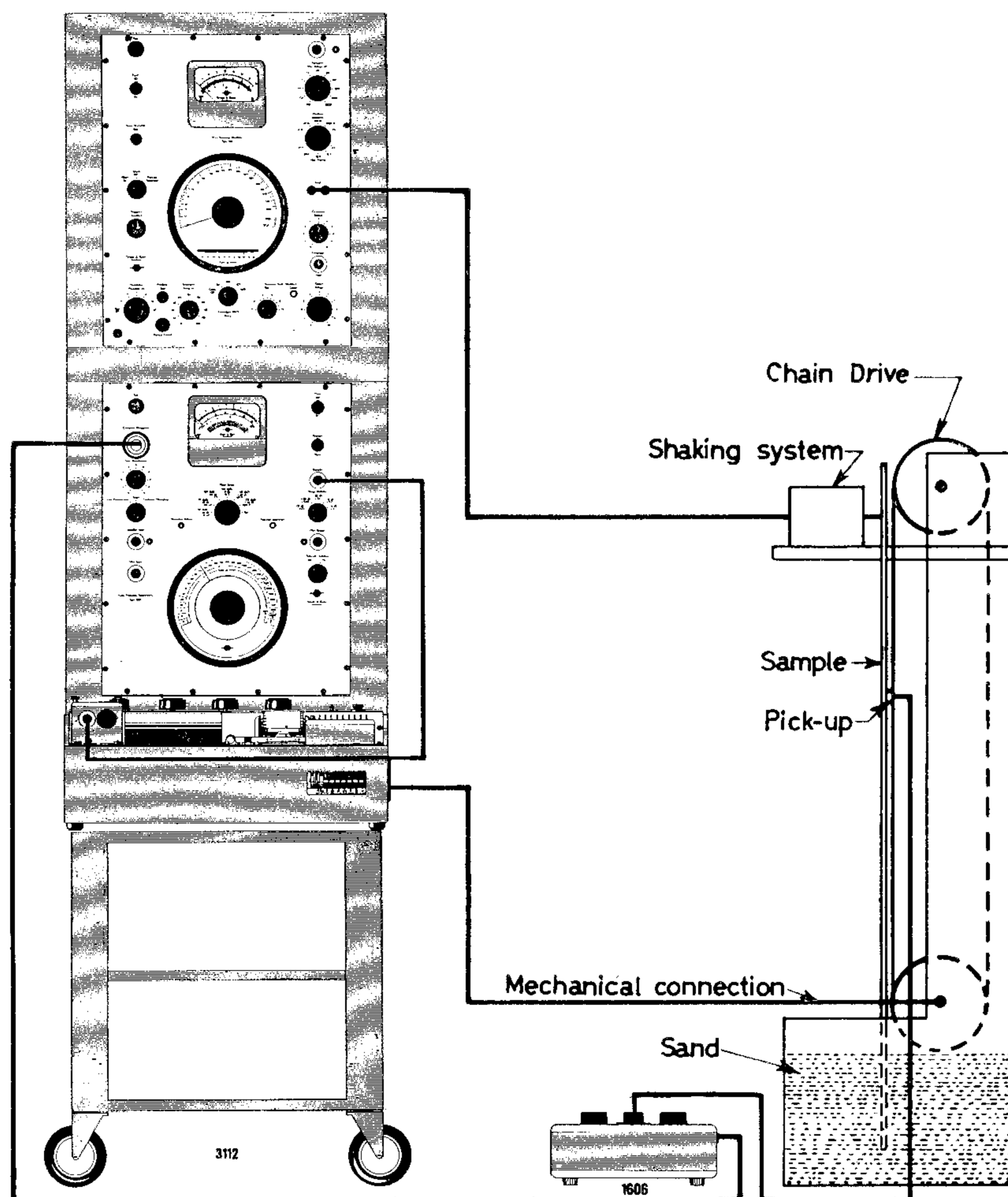


Fig. 22. Set-up used for the non-resonant method.

this type of selective measurement the signal to noise ratio is considerably improved relative to wide band measurements. Care must be taken, however, that the amplifier and the filter of the Spectrometer are not overloaded.

When the motor of the Level Recorder is started, the pick-up is automatically moved along the sample at a speed proportional to the paper speed of the Level Recorder.

Either a damped progressive wave or a standing wave pattern will now be recorded, depending on the value of the loss factor of the sample and on the impedance matching between the sand and the sample.

In fig. 23 a recording obtained with the described measuring set-up is shown.

The measurements were carried out on a bar shaped sample of plexiglas 2 mm thick and supplied with a 3.5 mm layer of putty on one side to produce a higher damping. From the standing wave pattern the modulus of elasticity and the loss factor are calculated, see also fig. 23.:

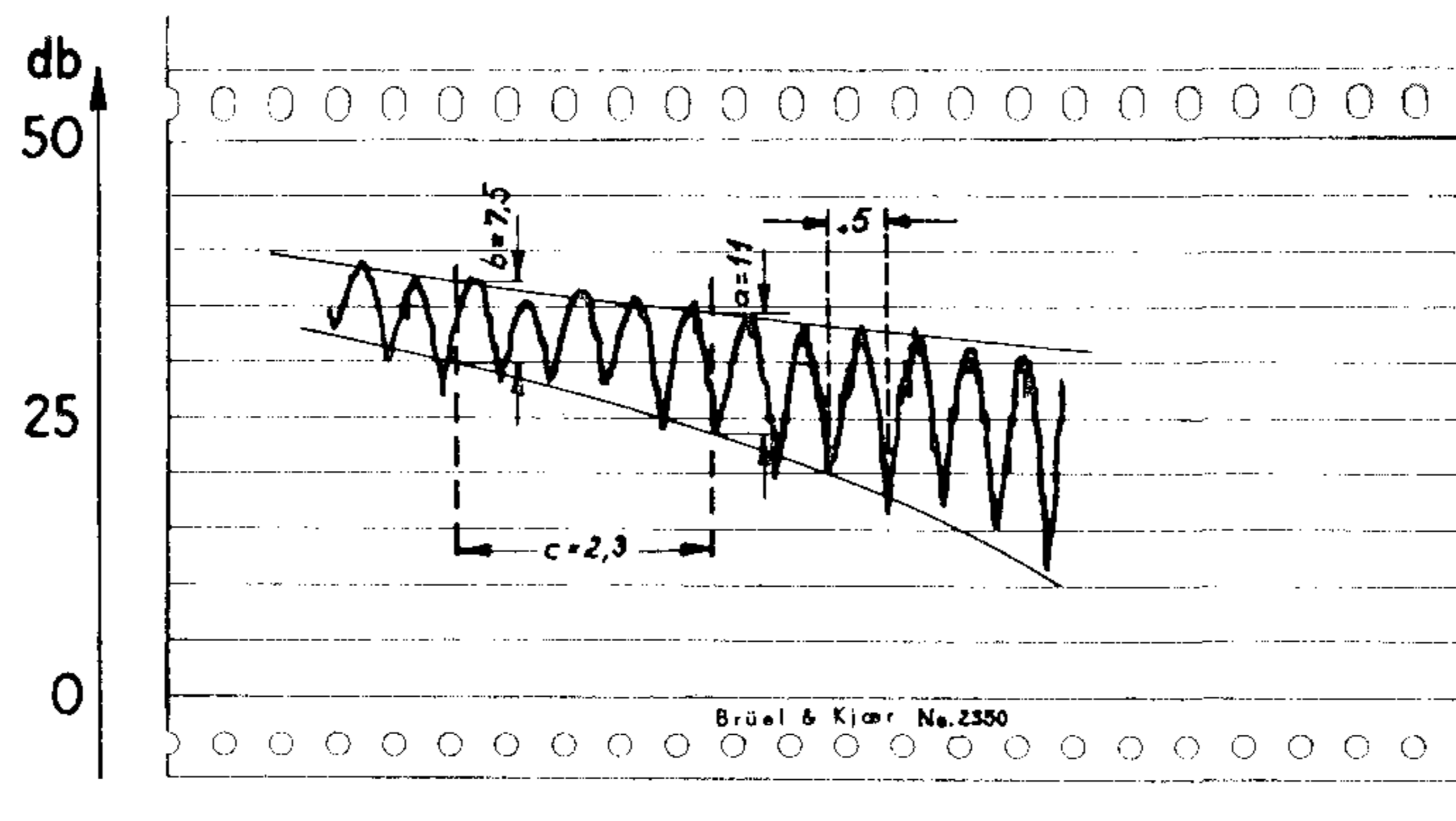


Fig. 23. Standing-wave pattern of a long plexiglas bar supplied with a layer of putty on one side.

$$a = 11 \text{ db, } b = 7.5 \text{ db, and } c = 2.3 \text{ cm}$$

and

$$D = \frac{a - b}{2c} = 1.52 \text{ db/cm}$$

from the equations

$$d = \frac{D \times \lambda}{13.6}$$

$$E' = \frac{3}{\pi^2} (f \times \lambda^2)^2 \frac{\rho}{q^2} \text{ dyne/cm}^2$$

is found

$$d = 0.11 \text{ and } E' = 1.9 \times 10^6 \text{ dyne/cm}^2$$

for $\lambda = 1.0 \text{ cm, } f = 1000 \text{ c/s, } \rho = 1.86 \text{ g/cm}^3 \text{ and } q = 0.55 \text{ cm.}$

Some Notes on the Equation $D = \frac{a - b}{2c}$

In fig. 24 is shown the exponential curve $A_1 e^{-\alpha x}$ corresponding to the amplitude of the incident wave, and $A_2 e^{\alpha x}$ corresponding to the amplitude of the reflected wave. Furthermore the sum $g_1(\alpha \xi)$ and the difference $g_2(\alpha \xi)$ of these curves are shown, all plotted to a linear scale. A new axis of abscissa (ξ) with reversed positive direction is introduced, having its zero point ($\xi = 0$) for $x = x_0$ where x_0 is the abscissa corresponding to the point of intersection between the curves $A_1 e^{-\alpha x}$ and $A_2 e^{\alpha x}$.

Transformed into this new system of coordinats the above functions are:

1. $f_1(\alpha \xi) = A e^{\alpha \xi}$
2. $f_2(\alpha \xi) = A e^{-\alpha \xi}$

and

$$3. \quad g_1(\alpha\xi) = f_1(\alpha\xi) + f_2(\alpha\xi) = A (e^{\alpha\xi} + e^{-\alpha\xi}) = 2A \operatorname{Cosh}(\alpha\xi)$$

$$4. \quad g_2(\alpha\xi) = f_1(\alpha\xi) - f_2(\alpha\xi) = A (e^{\alpha\xi} - e^{-\alpha\xi}) = 2A \operatorname{Sinh}(\alpha\xi)$$

Expressing the functions $g_1(\alpha\xi)$ and $g_2(\alpha\xi)$ as recorded on a logarithmic level recorder give, see also fig. 25:

$$3. \quad h_1(\alpha\xi) = 20 \log(k \times g_1(\alpha\xi)) = K + 20 \log(2A \operatorname{Cosh}(\alpha\xi))$$

$$h_2(\alpha\xi) = 20 \log(k \times g_2(\alpha\xi)) = K + 20 \log|2A \operatorname{Sinh}(\alpha\xi)|$$

where K is a constant dependant upon the measuring scale. The equation expressing the distance $\Delta h(\alpha\xi)$ between the two curves is consequently:

$$\Delta h(\alpha\xi) = h_1(\alpha\xi) - h_2(\alpha\xi) = 20 \log(\operatorname{Coth} \alpha\xi)$$

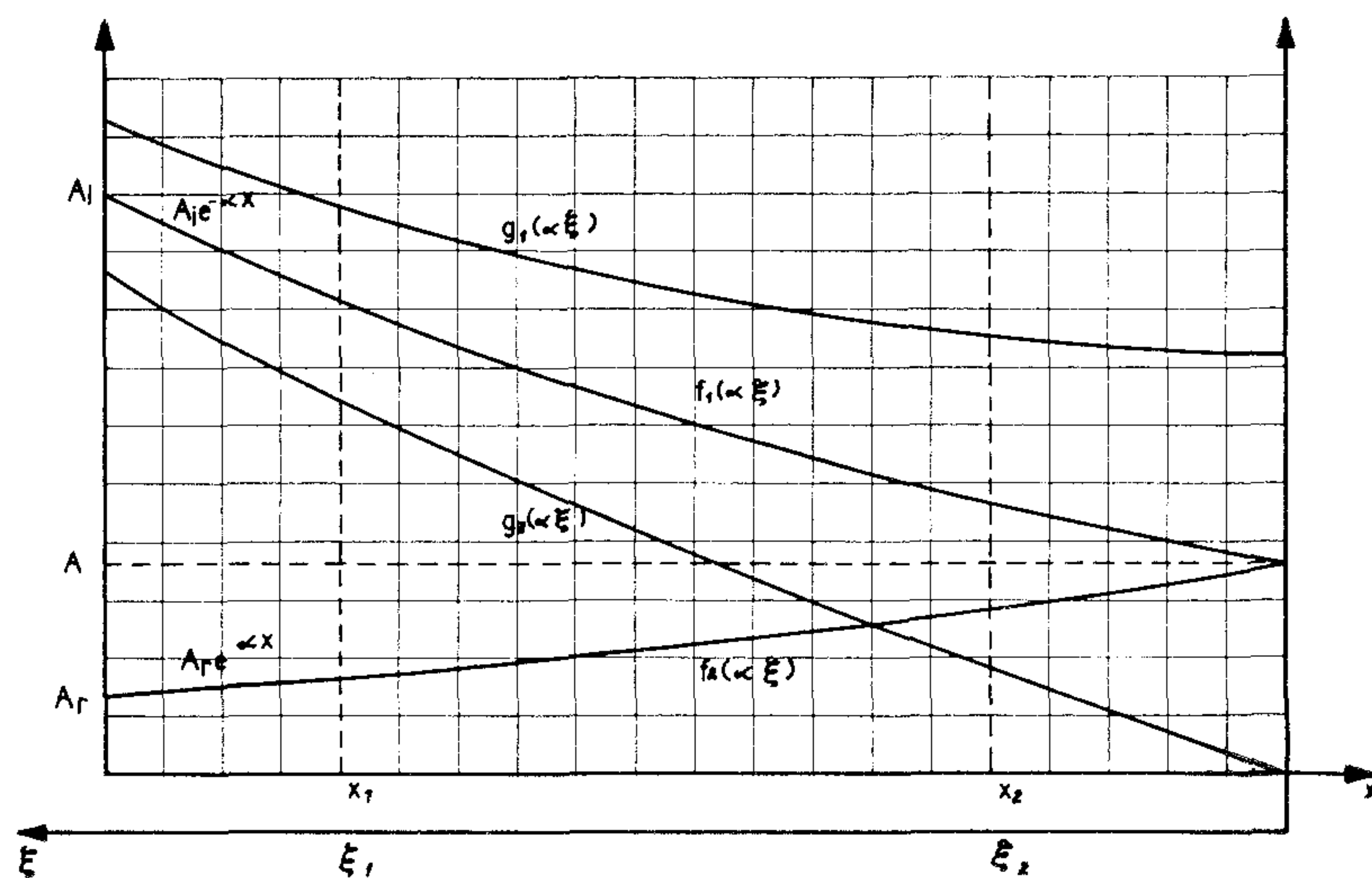


Fig. 24. Curves showing the damping of the incident and the reflected wave, and the sum and difference of these curves plotted to a linear scale.

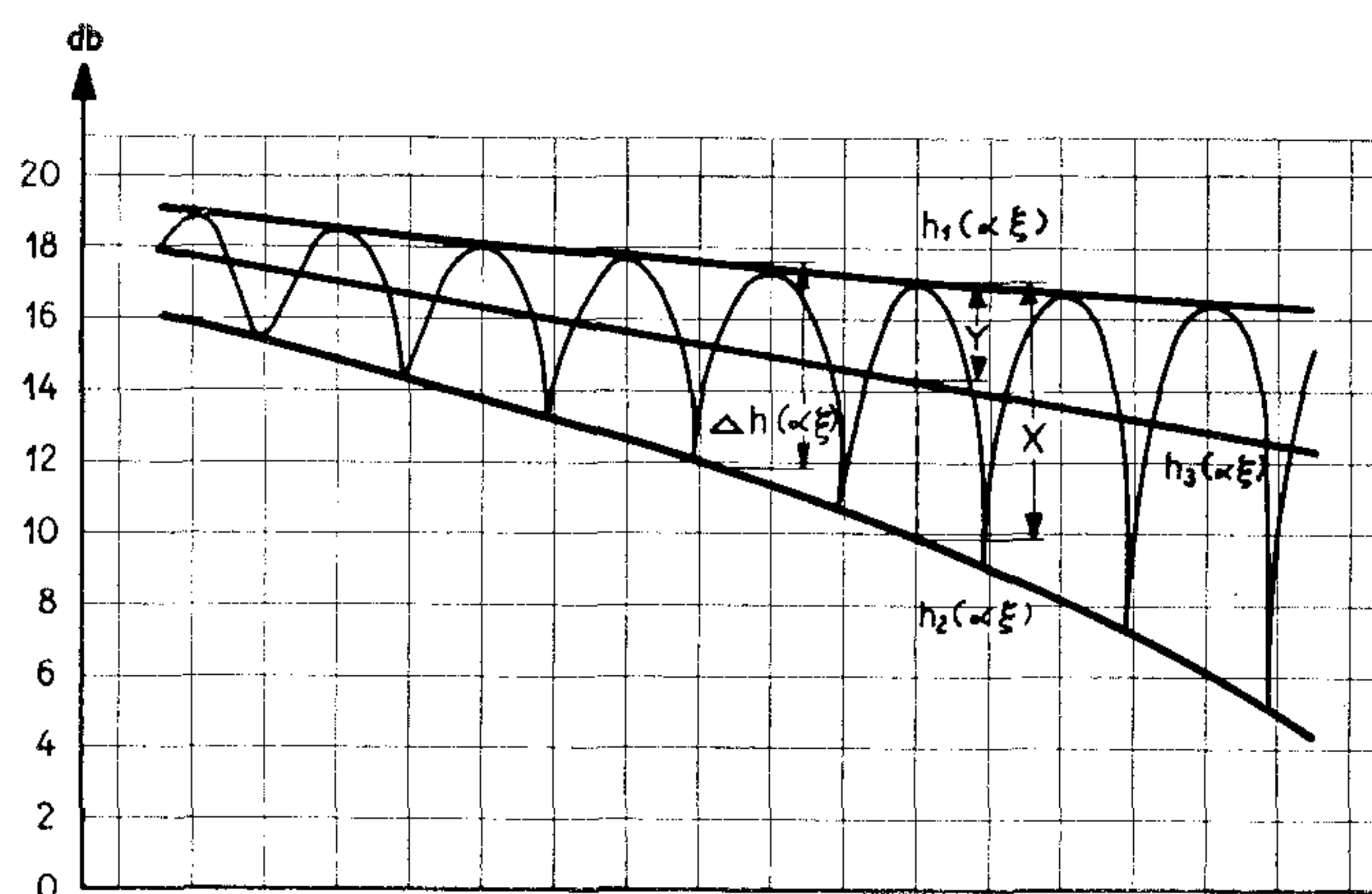


Fig. 25. A theoretic standing-wave pattern.

Under the assumption $0 \leq \alpha(\xi_1 - \xi_2) = \alpha c \leq 1$ is found

$$D = \frac{a-b}{2c} (\text{Sinh } 2 \alpha \xi_1) \text{ db/cm.}$$

In this equation $a = \Delta h(\alpha \xi_2)$ and $b = \Delta h(\alpha \xi_1)$.

It is thus seen that the equation $D = \frac{a-b}{2c} \text{ db/cm}$ is correct only for $\text{Sinh } 2 \alpha \xi_1 = 1$, which gives:

$$b = \Delta h(\alpha \xi_1) = 20 \log (\text{Coth } (\alpha \xi_1)) = 7.5 \text{ db.}$$

The equation $D = \frac{a-b}{2c}$ should therefore only be used in cases when $b = 7.5 \text{ db}$ and $\alpha c \leq 1$.

If these conditions cannot be obtained another procedure must be employed: The curves $g_1(\alpha \xi)$, $g_2(\alpha \xi)$ and $f_1(\alpha \xi)$ in fig. 24 are plotted to a logarithmic scale in fig. 25. From the figure is seen that

$$Y(\alpha \xi) = h_1(\alpha \xi) - h_3(\alpha \xi) = 20 \log (\text{Coth } (\alpha \xi)), \text{ and}$$

$$X(\alpha \xi) = h_1(\alpha \xi) - h_2(\alpha \xi) = 20 \log (\text{Cosh } (\alpha \xi)) - \alpha \xi$$

whereby the function $Y = F(X)$, which is shown in fig. 26 can be found.

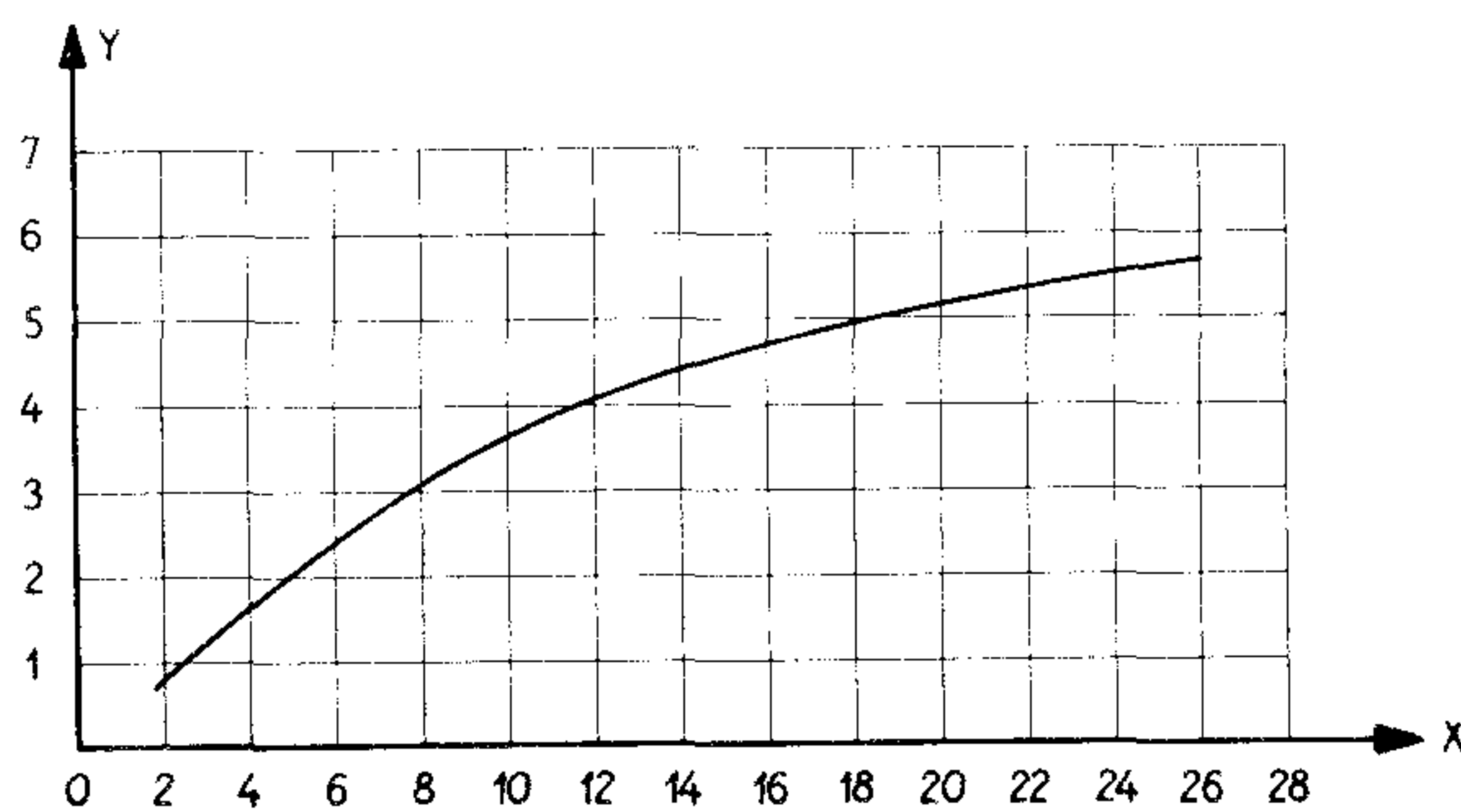


Fig. 26. Curve used for calculating $h_3(\alpha \xi)$.

It is now possible to draw the curve $h_3(\alpha \xi) = K_1 \xi + K_2$ on the recording paper. Because it is a straight line it is only necessary to know two points on the curve. The same recording as shown in fig. 23 is also shown in fig. 27 supplied with the curve $h_3(\alpha \xi)$. From this

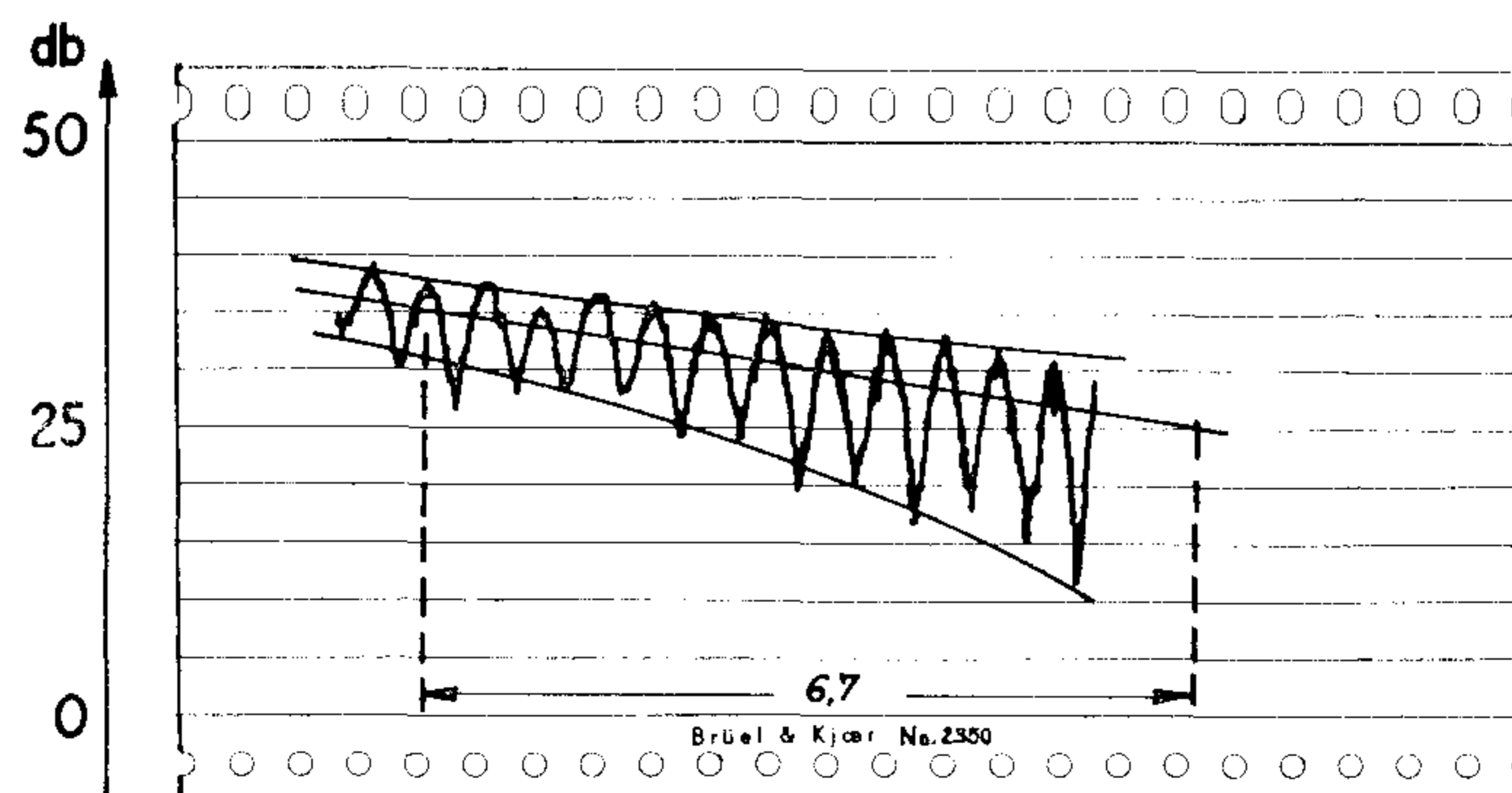


Fig. 27. The same standing wave pattern as shown in fig. 23. A 50 db potentiometer was used on the Level Recorder.

$$D = \frac{10}{6.7} = 1.49 \frac{\text{db}}{\text{cm}}$$

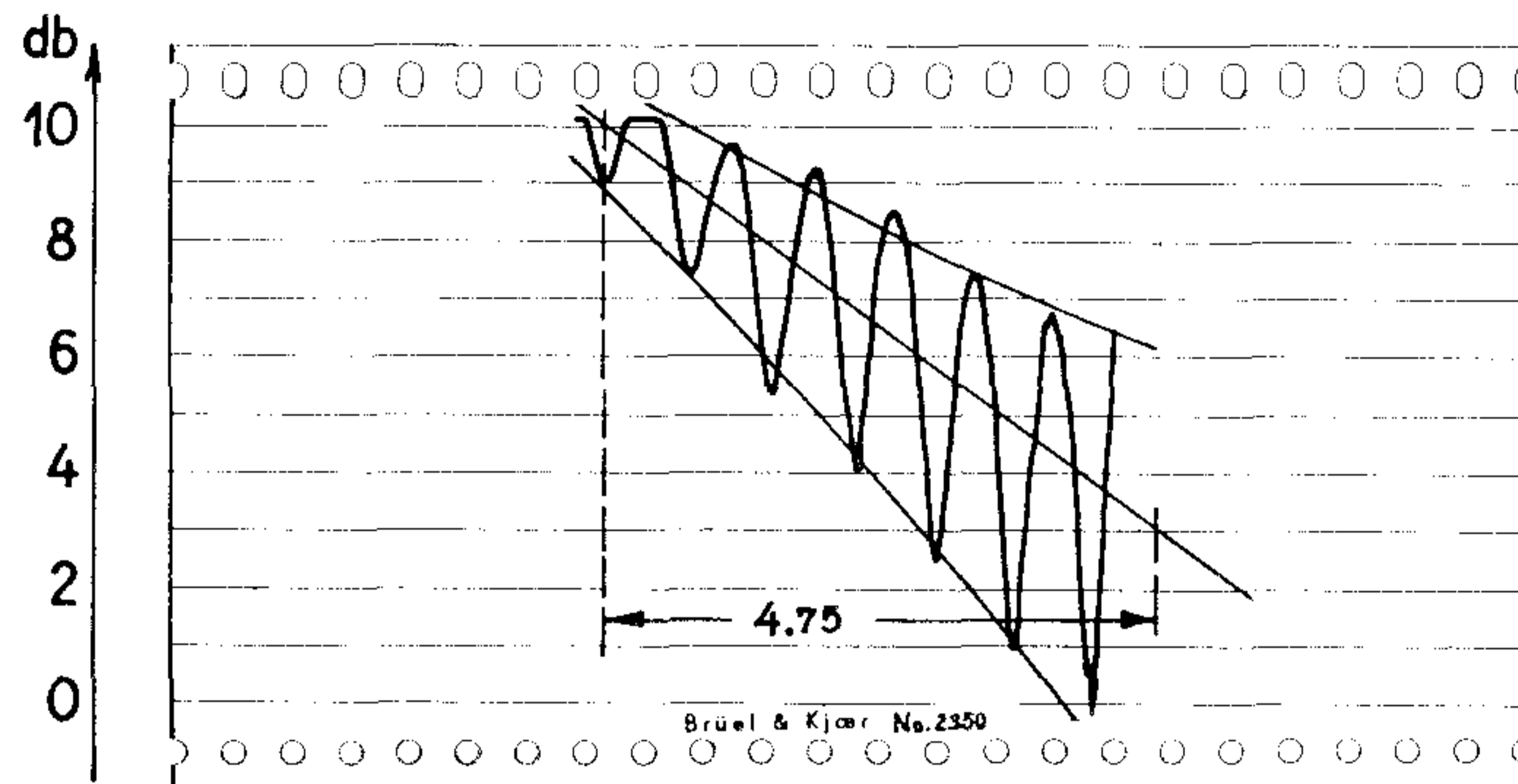


Fig. 28. Standing wave pattern recorded on the Level Recorder supplied with a 10 db potentiometer.

A recording obtained from measurements on the same material, using a 10 db potentiometer on the Level Recorder is shown in fig. 28. From the figure is found:

$$D = \frac{7}{4.75} = 1.48 \frac{\text{db}}{\text{cm}}$$

Conclusion.

From the foregoing text can be seen, that for measurements on materials with loss factors $d > 10^{-3}$ the "Frequency Response Method" is a very accurate laboratory measuring method. For $d > 10^{-3}$ the "Reverberation Method" is preferable and in production control systems the "Method Suitable for Small Test Objects" will be the most convenient one to use.

When measurements are carried out on non-homogenous materials which demand a larger sample than required when the "Method Suitable for Small Test Objects" is used the "Reverberation Method" offers a very profitable substitute to this method.

Literature.

1. Brüel & Kjær Technical Review No. 4 - 1957.
2. G. W. Becker: Mechanische Relaxationerscheinungen in nicht weichgemachten hochpolymeren Kunststoffen.
Kolloid - Zeitschrift Jan. 1955, Page 1—32.

News from the Factory.

New Instruments

Cathode Follower Type 2611.

The Cathode Follower Type 2611 which is shown in fig. 1 is a new design similar to the cathode follower used in connection with the Condenser Microphone Type 4111. It is supplied with a three meter long, multicore cable, with a sevenpole Microphone Plug JP 0017 fitting the Microphone input on the Brüel & Kjær instruments. Used in connection with the Microphone Cartridges MK 0001 and MK 0002 a Condenser Microphone of the hand-held type is obtained.

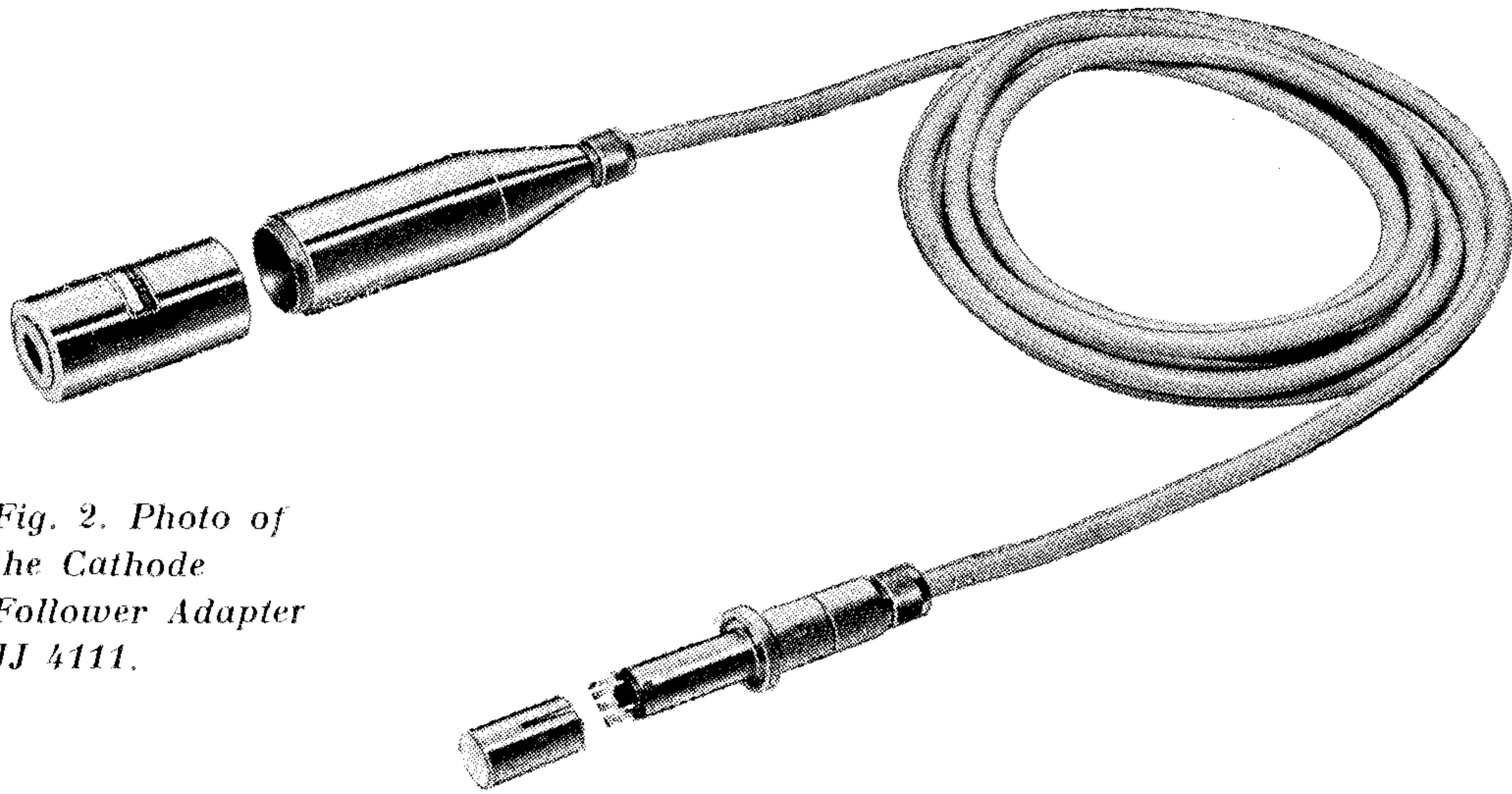


*Fig. 2. Photo of
the Cathode
Follower Adapter
JJ 4111.*

Fig. 1. Photo of the Cathode Follower Type 2611.

Cathode Follower Adapter JJ 4111.

In fig. 2 is seen the Cathode Follower Adapter JJ 4111. This Adapter, which is supplied with a normal screened Socket JJ 0014, is designed for use in connection with the Cathode Follower Type 2611 and the cathode follower of the Condenser Microphone Type 4111 for measurements of vibrations, substituting the Pre-amplifier Type 1606. To prevent the polarization voltage of the Cathode Follower to be supplied to the Accelerometer, the Cathode Follower Adapter JJ 4111 is supplied with a series capacitor of 5000 $\mu\mu$ F.

Brüel & Kjær

ADR. BRÜEL & KJÆR
NÆRUM - DENMARK



TELEPHONE: 80 05 00
BRUKJA, Copenhagen